

Document downloaded from:

<http://hdl.handle.net/10251/39803>

This paper must be cited as:

Macian Martinez, V.; Serrano Cruz, JR.; Dolz Ruiz, V.; Sánchez Serrano, J. (2013).
Methodology to design a bottoming Rankine cycle, as a waste energy recovering system in
vehicles. Study in a HDD engine. Applied Energy. 104:758-771.
doi:10.1016/j.apenergy.2012.11.075.



The final publication is available at

<http://dx.doi.org/10.1016/j.apenergy.2012.11.075>

Copyright Elsevier

Methodology to design a bottoming Rankine cycle, as a waste energy recovering system in vehicles. Study in a HDD engine

V. Macián, J. R. Serrano, V. Dolz, J. Sánchez

Universitat Politècnica de València, CMT-Motores Térmicos, Camino de Vera s/n, 46022 Valencia, Spain.

Abstract

This article describes a methodology for the optimization of a bottoming cycle as a waste heat recovering system in vehicles. The methodology is applied to two particular cases in order to evaluate the preliminary energetic and technical feasibility of the implementation of a bottoming cycle in a heavy duty diesel (HDD) engine considering two different criteria. Initially, a study of the different waste heat sources of the engine is described. In this study, the power and exergy of each heat source is quantified, in order to evaluate which sources are suitable to be used in the bottoming cycle. The optimum working fluids to run the cycles are selected (water and R245fa). Then, the ideal Rankine cycle is optimized for the two different working fluids and different sets of heat sources (all the available heat sources and the sources with high exergy respectively) throughout the engine operating range, reaching a maximum improvement of 15 % of the fuel consumption of the engine. Later, a study of the minimum temperature difference between the hot and cold flow of the heat exchangers is described. The improvements in fuel consumption and the size of the installed heat exchanger are related to this temperature difference. Finally, the non-ideal behavior of the machines (pump and expander) is analyzed, obtaining a maximum improvement of 10 % in brake specific fuel consumption (*bsfc*).

Keywords: Organic Rankine Cycle, Diesel, Rankine Cycle, Recover Waste Power

1. Introduction

The interest for increasing fuel economy and efficiency has recently been growing among governments, industrial companies and engine manufactures to the extent that the quantity of waste energy produced [1], represent a driving force for development of more effective methods of waste energy recovery [2]. The carbon dioxide emissions are also gaining significant attention due to its association with global warming and the fact that about 80 % of said emissions in the Organization for Economic Co-operation and Development (OECD) countries or the European Union are due to the use and production of energy, industries or manufacturing [3, 4]. Nowadays, the global carbon dioxide emissions have risen steadily over the past 50 years to a concentration of approximately 380 ppm in the atmosphere as of 2006 [5].

*V. Dolz. CMT-Motores Térmicos, Universitat Politècnica de València, Camino de Vera s/n, 46022 Valencia, Spain.
Phone: +34 963877650 Fax: +34 963877659 e-mail: vidolrui@mot.upv.es

10 A large number of solutions have been proposed to generate electricity from low temperature waste heat sources
11 and are now applied to such diversified fields as solar thermal power, geothermal, biomass and industrial waste heat.
12 Among the proposed solutions, the implementation of a bottoming cycle currently is one of the most studied options
13 [6, 7]. Among the different solutions, Rankine Cycle (RC), Organic Rankine Cycle (ORC), Stirling cycle (SC) and the
14 Brayton Cycle (BC) can be analyzed in order to find the one generating the largest power. The RC and ORC solution
15 is considered by Bianchi *et al.* [8] as the more profitable configuration for converting the low-grade power into the
16 higher output power. Many theoretical investigations have been performed in order to design the optimum cycle
17 (working fluid, evaporator and condenser pressure, superheating temperature, choice of the expander, etc.) taking into
18 account the heat source characteristics [9–15].

19 One of the largest sources of waste energy is the internal combustion (IC) engine used in different vehicles (naval
20 ship, railway, automotive, etc) as shown in the Eurostat publication in 2011 [16]. The IC engine converts approxi-
21 mately one third of the combustion power into mechanical power. The remaining power is distributed to different heat
22 exchangers or is directly released to the ambient (exhaust gases). As a result, an IC presents various waste heat sources
23 with a wide range of temperature and exergy levels [17–19]. Additionally, the waste heat sources vary considerably
24 depending on the engine operating point [20]. Therefore, the preliminary design of the optimal solution is usually
25 not an easy task [21, 22]. Therefore, the published articles on this topic focus on different factors about this complex
26 problem. In this paper, the problem of designing a bottoming cycle to recover the energy of waste heat sources in an
27 IC engine is addressed generally. Consequently, this work considers all these partial issues studied in other articles as
28 parts, integrating them in a general methodology and considering the influence of these partial topics in the obtained
29 final result.

30 The methodology discussed in this paper is a comprehensive theoretical study for simplifying the complex problem
31 of the waste heat source recovery system in vehicles. This methodology implies the evaluation of all the heat sources
32 at each operating points and selection of the waste heat sources. It then applies an iterative-parametric optimization
33 procedure in order to calculate the optimum working fluid and cycle conditions based on the maximum power output
34 cycle for each operating points taking into account various restrictions as space requirements limitations, maximum
35 expansion ratio etc.,. The methodology is also applied to a bottoming cycle for a Heavy Duty Diesel (HDD) engine with
36 a two-stage turbocharging system, from which experimental data are available. The resulting power balance was used
37 to propose an optimal configuration for the most frequent combinations of speed and load engine conditions (operating
38 engine points) [23]. The goal of this paper is to develop a general theoretical methodology in order to evaluate the
39 maximum power and sizing of the system (energetic and technical feasibility) of the different configurations and show
40 valuable results for the remaining problem of the waste heat power recovery in IC engines.

2. Methodology

The design of the implementation of a heat power recovery system in a vehicle is complex due to numerous restrictions (maximum pressure ratio in the expander, condensation temperature, minimum temperature difference between hot and cold source, etc) or goals (reduction of fuel consumption, maximum output power, space limitations, etc) that must be considered. Sometimes the selection of the waste heat sources in a bottoming cycle for a vehicle constitutes the key part of the design process. Two important criteria are associated with this selection: the power output and the space requirements of the cycle. The more wasted heat to recover, the higher the power output and heat exchanger volume. Once the waste heat sources are selected, the design calculations are essentially a series of iterative calculations made on the preliminary design until a satisfactory solution is achieved. In these calculations, different working fluids, the effect of the different irreversibilities and other additional restrictions are considered in order to define a preliminary design of the heat recovery system.

In this section, a methodology is proposed in order to simplify the process of the selection of the best configuration of a bottoming cycle by taking into account different initial limitations and goals. The proposed methodology consists of the following steps, also shown in Figure 1:

1. Specification of the problem. In this first step, the goals and limits of the bottoming cycle are fixed. The goals must be satisfied by all the steps followed in the methodology. The limits must be imposed in the cycle in order to obtain the cycle output power.
2. Evaluation of all the waste heat sources, in order to identify the sources with higher heat power level and better recoverability, using energetic and exergetic studies.
3. Selection of the waste heat sources. The most suitable heat sources are selected depending on their exergetic qualities, in order to use the best heat sources in the next studies. In this step, the available heat power in the selected sources must be higher than the minimum power output objective. If the total waste heat power is less than this requirement, the design problem has no solution. However, fewer heat sources used in the process imply more compact heat exchangers in the cycle, a less complex control of the cycle and it can produce a higher efficiency.
4. Selection of the working fluid. Several working fluids commonly used in bottoming cycles are considered in order to define those which produce the maximum cycle output power in the following step.
5. Calculation with the ideal cycle assumption. The working fluid selected and the limits detailed in the first step are imposed in order to evaluate the ideal configuration for each operating point. Isentropic compression and expansion processes and zero pressure drops in tubes are imposed in this ideal study. If the power output obtained in the solution does not satisfy the power specification, the working fluid and/or heat sources selected will have to be reconsidered. If not, the design problem has no solution.
6. Sizing of heat exchangers. The size of the heat exchanger in the optimum ideal cycle configuration is calculated through the heat transfer needed, the pressure drop allowed and the minimum temperature difference between

75 the working fluid and the engine waste heat sources (dT). The heat exchanger volume must satisfy the space
76 requirement imposed. The dT must be reconsidered when the heat exchanger volume does not satisfy the
77 volume requirement.

78 7. Calculation of the real cycle. Non-isentropic compression and expansion processes are calculated in this point of
79 the theoretical study. Different charts are used to estimate the pump and expander machine efficiencies [24, 25].
80 If the power output obtained in this step is lower than the minimum power required, the selection of working
81 fluid and/or heat sources will have to be reconsidered. In this step, the effect of the real cycle assumption on the
82 heat exchanger sizing is neglected.

83 8. Other pre-imposed limits and goals must be evaluated before determining the final optimum configuration. In
84 this last step, other feasibility criteria such as: maximum installation cost or weight could be evaluated before
85 determining the optimal bottoming cycle configuration.

86 Following, two examples are shown in next section in order to illustrate the effect of each step on the performance
87 of a bottoming cycle for a double-stage HDD engine.

88 3. Application of the methodology for bottoming cycle in HDD engine

89 Recovering waste energy in an automotive is one of the most complex cases in the implementation of a bottoming
90 cycle in vehicles due to four main aspects: 1) There are many operating points, 2) in each operating point there are
91 different available waste heat sources, 3) these sources present very different temperature levels and power available,
92 4) the limitation and goals are usually very strict because the solution implemented must be cheap, without large space
93 and weight requirement, technically feasible and profitable in global energetic terms. In this section, the problem of
94 the implementation of a bottoming cycle in HDD Engine is selected for the purpose of illustrating the methodology
95 detailed previously.

96 3.1. Problem specification

97 In a vehicle, the reduction of bsfc (brake specific fuel consumption) can be considered as the most important goal
98 of the implementation of this kind of technology. A high power output in a bottoming cycle implies an important heat
99 transfer process. This heat transfer process requires different heat exchangers whose volume and weight requirements
100 can be higher than allowed by the vehicle design limits. Taking this restriction into account, the methodology was
101 applied following two different goals as examples:

- 102 • Maximum reduction of brake specific fuel consumption ($bsfc$) without any space limitation, here in after, case
103 **A**.
- 104 • Acceptable reduction of $bsfc$ with the space restriction, here in after, case **B**. In this work, a $bsfc$ higher than 5
105 % and space requirement lower than $0.2 m^3$ were imposed. The imposed goals or restrictions strongly depend
106 on the engine manufacturing criteria.

107 The limits of the problems were fixed as:

- 108 • The pressure ratio in the expansion machine must be lower than 25 to achieve an efficient expansion process.
- 109 • Initially, the proposal cycles minimum temperature difference in the heat exchange processes is fixed to 10°C
110 [26–28].
- 111 • The working fluid in the condenser had to be cooled by the ambient. These conditions were fixed in 40°C and
112 1 bar.

113 The engine used in this study was a 12 litre double-stage turbocharged HDD [29]. The maximum engine torque is
114 2100 Nm and this values is achieved at 1000 rpm and 100% load and the maximum engine power is 311 kw at 1800
115 and 100 % load. The HDD has been adapted according to the anti-pollution directive (US2007) [23].The scheme of
116 the engine is shown in Figure 2.

117 The engine is placed in a test bench with an electric brake which allows steady tests under different operational
118 conditions. The engine is also instrumented to measure torque, engine speed, fuel consumption, air mass flow in the
119 intake line, pressures and temperatures in the compressors and turbines. The blow-by effect is neglected, for this, the
120 exhaust gases mass flow is calculated as the sum of intake mass flow and fuel consumption flow. The waste power of
121 the exhaust gases is calculated using the measured temperature and the estimated mass flow. The waste power of the
122 remaining heat sources have been calculated measuring the inlet and outlet temperatures and coolant mass flow in the
123 cylinders (radiator) and the rest of heat exchangers (EGR cooler, intercooler and aftercooler).

124 Eleven steady operating points of the engine have been chosen for testing and there after, to design and simulate
125 the recovery cycle. These points represent the steady-state engine test modes with defined speed and load used by the
126 directive (US2007) for the evaluation of the emission [23]. Table 1 lists these operational points.

127 3.2. Evaluation of the heat sources

128 Analyzing the wasted power in the thermal engine to identify the main waste heat sources is the second step
129 of this methodology. These sources are located in: 1) the exhaust gases 2) the EGR coolers, 3) the intercooler, 4)
130 the aftercooler and 5) the engine cooling water. The heat power in these sources is calculated using mass flow and
131 temperature measurements. The available power between the inlet and outlet conditions (1 and 2) of each source is
132 calculated considering the gases as ideal and perfect gases, Equation (1):

$$E_{flow} = \dot{m}_{flow}(h_1 - h_2) = \dot{m}_{flow}C_p(T_1 - T_2) \quad (1)$$

133 where C_p has been considerate 1 kJ/kgK and 1.15 kJ/kgK for fresh air and combustion gases respectively. The
134 ambient conditions are considered as the reference state.

135 The energetic levels of the waste heat sources for two different engine operative points are listed in Table 2: 1800
136 rpm-100% load and 1200 rpm-25 %. These points were selected for two reasons: 1) They are points with energetic

137 level distributions very different and 2) The maximum reduction of brake specific fuel consumption will be achieved
 138 in these operative points for the two cycles studied in this paper. The total waste power of the engine (summarizing all
 139 the heat sources) is represented in the engine map (Figure 3). The contour lines in Figure 3 were created on the basis
 140 of the eleven engine operating points. The Kriging interpolation method [30] was applied on all contour lines of the
 141 figures in the paper using a surface mapping software (SURFACE v8.0) [31]. Figure 3 shows that the available power
 142 increases with the crankshaft speed and the engine load. The highest waste heat power corresponds to the 1800 rpm
 143 and 100% load, because this is the point where the most fuel is injected. While 600 rpm and 0% does not practically
 144 generate any waste heat.

145 The waste heat power of the HDD engine is up to 420 kW. But this power can be used to improve the engine
 146 efficiency if it is converted into mechanical work. The exergetic study of these waste heat sources can evaluate which
 147 is the maximum obtainable work in each engine operating point. The exergy represents the maximum work that can
 148 be extracted from a thermodynamic cycle from an initial state (state 1) to an environment state (state 0). Thus, the
 149 exergy is obtained as Equation (2) shows:

$$Ex_{flow} = \dot{m}_{flow} \left((h_1 - h_0) - T_0(s_1 - s_0) \right) \quad (2)$$

150 In this way, the exergy variation between two states (from 1 to 2) with the same environmental conditions can be
 151 obtained as Equation (3) shows:

$$\Delta Ex_{flow_{1-2}} = \dot{m}_{flow} \left((h_2 - h_1) - T_0(s_2 - s_1) \right) \quad (3)$$

152 The exergies of the waste heat sources considered in this study can be calculated as a total exergy (exhaust gases)
 153 using Equation (2) or as variation of exergy (intercooler, aftercooler, EGR and cooling water) using Equation (3). The
 154 exergetic levels of the waste heat sources at 1800 rpm -100 % load and 1200 rpm and 25 % load are listed in Table 2
 155 Adding all these wasted exergies, the total waste exergy can be calculated. Figure 4 shows this total waste exergy on
 156 the engine map.

157 When the results are analyzed in terms of exergy, we can state that a third of the total waste power could be
 158 converted into mechanical power by a thermodynamic cycle, if the external and internal irreversibilities are not con-
 159 sidered.

160 It is worth noting that in a thermodynamic cycle, the highest exergy destruction will further mainly take place
 161 during the heat transfer process in the heat exchangers. The greater the temperature difference between the cooled
 162 fluid and the heated fluid, the greater the exergy destruction [32–35]. On the other hand, this temperature difference
 163 will depend strongly on the selected working fluid

164 3.3. Selection of the waste heat sources

165 The third step is the selection of the waste heat sources. The selection process depends on the goals and limitations
 166 fixed in the specification problem (first step). To illustrate the methodology exposed in this paper, two different

167 selections of the heat sources will be carried out the **A** and **B** problem criteria. Each waste heat source in a HDD
168 engine has a different temperature, exergetic and energetic level. These differences can produce significant variations
169 in the cycle efficiency and consequently in the cycle net power [21, 22]. The variations in the cycle efficiency occur
170 because the temperature of the heat source determines the evaporator temperature of the cycle and the evaporator
171 temperature is directly related to the cycle efficiency. The exergy contribution of each waste heat source has been
172 studied to select the best sources in the engine (generally those sources with highest temperature), in order to address
173 step (2) of the proposed methodology in Figure 1. The exergy contribution of EGR, exhaust gases and aftercooler
174 is shown in Figure 5. These three heat sources account for nearly 80% of the total exergy in the engine. Thus, the
175 implementation of a bottoming cycle with these waste heat sources is highly recommended in order to simplify the
176 bottoming cycle structure.

177 Two different sets of heat sources have been considered in this study: The first configuration for the case **A**
178 includes all the HDD Engine waste heat sources, in order to evaluate the maximum output power obtained at each
179 engine working condition. The second option for the case **B**, considers only the three higher exergetic sources (exhaust
180 gases, EGR and aftercooler).

181 3.4. Selection of the working fluid

182 One of the factors regarding the efficiency of a bottoming cycle is the selection of the optimum working fluid
183 [36, 37]. For this study, different fluids like halocarbons, CFC, HCFC, HFC, Hydrocarbons, ammonia and water have
184 been considered as possible working fluids. These fluids were analyzed in previous works with the same HDD engine
185 studied in this paper for different bottoming cycles by Dolz *et al.* [21] and Serrano *et al.* [22]. The criteria used for the
186 selection of the working fluid are good physical and thermodynamic characteristics providing high thermal efficiency
187 and high exploitation of the available heat source. Furthermore, the selected fluid should be environmentally friendly,
188 present low toxicity and characteristics of low-zero inflammability. In these works, water and R245fa were considered
189 as the optimum working fluids.

190 A RC with water as working fluid has acceptable exergy losses in heat exchanges of high-temperature sources
191 [38] due to it presents a low temperature difference through the heat transfer process [39]. because it allows a low
192 temperature difference between cooled and heated fluids. The R245fa is an organic fluid in an ORC; it is often used
193 in these cycles, in order to recover the power from heat sources at low temperatures,[7, 9, 38, 40, 41]. RC with water
194 and ORC with R245fa will be the studied bottoming cycles to recover the waste heat in different engine working
195 conditions for both cases (**A** and **B**). More details of this justification can be found in [21, 22], where a deep analysis
196 of this selection was performed only for 1800 rpm and 100% load engine operating conditions.

197 3.5. Calculation with the ideal cycle assumption

198 In step (5) of the proposed methodology, the performance of an ideal cycle in each engine operating point was
199 evaluated in order to analyze which had the maximum output power through the implementation of a power cycle. The

200 thermodynamics properties of the working fluid are calculated by REFPROP NIST 7.0. A parametric-iterative method
201 has been employed to choose the optimum working fluid mass flow, vaporization and superheating temperatures for
202 each operating point. This method was fully described by Dolz *et al.* [21] for the configuration with all sources at
203 1800 rpm and 100 % with the same case engine. The main goal of the study was to maximize the power output of the
204 cycle while keeping the engine working conditions constant. Therefore, the increase of power output by the bottoming
205 cycle is shown as a reduction of *bsfc* by the IC engine. Thus, the main goal of the study was to minimize this variable.

206 The hypothesis assumed in this analysis was:

- 207 • Isentropic efficiencies for the expansion machine and pump processes in this ideal study are 100%.
- 208 • Heat losses in the cycle are not considered.
- 209 • The waste sources were recovered from lowest to highest temperature level. The cooling water heats up the
210 working fluid to saturated fluid. The cooling water, intercooler, aftercooler, exhaust gases and a part of the
211 EGR heat was employed in the evaporator. The rest of EGR heated up the saturated vapor to superheated vapor.
212 Details and thermodynamic diagrams of these processes for the 1800 rpm and 100% load can be found in [21].

213 The first theoretical study (case A) deals with the implementation of a thermodynamic cycle that allows recovering
214 all the waste heat sources of the engine. Figure 6 shows a countour lines of the reduction of *bsfc* obtained at each
215 engine operation point by the implementation of a RC (water cycle) and an ORC (R245fa cycle). In both configura-
216 tions, a significant reduction of *bsfc* was achieved: from 15% to 5% for RC and from 12% to 5% for the ORC. The
217 area near 1200 rpm is the most frequent operating zone in this HDD engine and this is also the zone with a higher
218 improvement in *bsfc*. Some of the bottoming cycle operating conditions in case (A) configuration are listed in Table
219 3. At low speed (800-1000 rpm) and full load points, the EGR rate is zero. So, the exhaust gases are used to heat up
220 the saturated vapor to superheated vapor in these points.

221 In the configuration with all the heat sources (case A), a low temperature difference between the evaporator and
222 condenser is imposed, in order to recover the waste heat sources that have lower temperature, i.e. 80 °C-95 °C for the
223 cooling water.

224 The large dissipated heat in the heat-exchangers and the complex control system are two drawbacks to implement
225 the case A configuration.

226 The same procedure was followed for the case B configuration. Figure 7 shows the results of this study. Table 3
227 lists the bottoming cycle conditions for two engine operative points (1800 rpm- 100 % load and 1200 rpm and 25 %
228 load.

229 The ORC configuration has a similar behavior as in the previous case but with a lower reduction of *bsfc* ranging
230 from 10% (at 1200 rpm and 25% load) to 3% (at 800 rpm and 100 % load). This similarity is due to the optimum
231 cycles because the superheating temperatures in ORC can not achieve a excessively high level (close to 150 °C) as
232 shown Table 2. But the available waste heat power was lower, because the heat power of the sources has decreased.

233 The main differences were observed in the RC implementation. In this configuration with the high temperature
 234 sources, the cooling water temperature does not imply a restriction in the evaporation temperature. For this reason,
 235 higher evaporation and superheating temperatures as shown in Table 3 can be considered for the optimal cycle, for
 236 instance, at 1800 rpm and 100 % load the superheating temperatures is close to 500 °C. Consequently, the reduction
 237 of *bsfc* ranged from 10% to 14% at points of high thermal level (high speed and load), i.e. from 1200 to 1800 rpm and
 238 100% load. The highest reduction of *bsfc* was achieved at 1800 rpm and 100% load.

239 3.6. Sizing heat exchangers

240 The technical implementation of a bottoming cycle in a HDD engine is not only based on thermodynamic de-
 241 sign criteria. Also, the required space, weight and cost of installation are important criteria for the viability of the
 242 considered solution. Thus, the sizing and the materials of the heat exchangers for the power cycles proposed in the
 243 theoretical study are calculated. This involves the selection of heat exchanger construction type, flow paths, physical
 244 size to meet the specified heat transfer and pressure drops within specified constraints [42]. For the sizing of the heat
 245 exchangers, the following criteria have been imposed:

- 246 • Aluminum was selected as the heat exchanger material.
- 247 • The heat exchangers were designed so that the pressure drop is less than 2%, in order to be consistent with the
 248 hypotheses considered in the previous step.
- 249 • Shell&tube heat exchangers have been chosen for the gas-liquid and liquid-liquid heat transfer. For the rating
 250 problem, the step-by-step developed by Delaware-Bell *et al.* [43] has been followed. An E-11 shell flow ar-
 251 rangement with a square pitch configuration is selected for all the shell& tube exchangers [44]. The number of
 252 passes and the log mean temperature difference correction factor F have been calculated using the Domingo's
 253 correlation [45]. The Dittus-Boelter's correlation for the heat transfer coefficient and Blasius/McAdams equa-
 254 tions for the friction factor were used for the calculation in the tube side [46]. The ideal heat transfer coefficient
 255 for the shell side was calculated by:

$$h_{id} = \frac{jC_p G_s (\Phi_s)^n}{Pr^{\frac{2}{3}}} \quad (4)$$

256 where the term j is the ideal Coulburn factor for the shell side and can be determined form the appropriate
 257 Bell-Delaware curve for the tube and pitch [43], C_p is the average fluid heat capacity at constant pressure along
 258 the heat transfer process, G_s is the shell side mass flow velocity, the term (Φ_s^n) is the viscosity correction factor,
 259 with accounts for the viscosity gradients along the tube wall versus the viscosity at the bulk mean temperature
 260 of the fluid and Pr is Prandtl number. The standard definition of this variable is given by Equation 5 taking into
 261 account the different temperature criteria for the gases and liquids being cooled or heated [47]:

$$(\Phi_s)^n = \left(\frac{\mu}{\mu_w}\right)^{0.14} \quad (5)$$

The correction factors J of the heat transfer coefficient in the shell side have been neglected. The heat transfer coefficient for the boiling process is calculated by the approach developed by Bromley *et al.* [48], it is used to predict the film boiling heat transfer coefficient for a horizontal tube. The heat transfer correlation used for internal condensation in horizontal tubes is proposed by Carey [49] and Ould Didi *et al.* [50]. The overall pressure drop due to the evaporation process was obtained by the Martinelli-Nelson's correlation [51]. The data on fouling factors were given by Ludwig [52]. The both side fouling factor was fixed to $0.0003 \text{ m}^2 \text{ }^\circ\text{C}/\text{W}$.

- Single-pass crossflow plate-fin exchangers have been chosen for the gas-vapor heat transfer. A similar step-by-step method for rating the single-pass crossflow plate-fin exchanger is used in order to obtain following information: Reynolds numbers, surface basis characteristics, corrections to the surface basic characteristics due to temperature-dependent properties, heat transfer coefficients and fin efficiencies, wall thermal resistance and overall thermal conductance, NTU, exchanger effectiveness, heat transfer rate and pressure drops on each fluid side [42]. The condenser is placed the behind the grille and cooled directly by the ambient. The vehicle speed is fixed at 90 km/h due to its frequent occurrence as road truck speed, irrespective of the load and engine speed.

The operating points with greater reduction in *b_{sfc}* for each configuration studied were considered in order to evaluate the space requirement. Table 4 shows the selected operating points with $dT=10^\circ\text{C}$ (from **1i** to **4i**). The dimensions and pressure drops required of the heat exchanged designed are listed in Table 4.

Figure 8 shows the heat exchanger volume obtained by using the previous criteria. The evaporator is the biggest heat exchanger in the RC and the ORC configurations of case **A** (Point **1i** and **2i**), due to the large heat transfer that takes place during the evaporation process. The heating process during the liquid phase presents a low heat exchange, because the working fluid at the pump outlet is near to the saturation curve. The volume of the evaporator in case **A** is also high enough to allow such a high heat exchange rate without a high pressure drop in the shell side. The evaporator absolute pressure in the RC configuration with all the heat sources (**1i**) is above 0.3 bar. This implies that the heat exchanger must be designed with a large diameter and extreme length in order to avoid a high relative pressure drop as shown Table 5. This effect is less important in the ORC (**2i**), because the evaporator pressure is higher and the relative pressure drop is lower. The superheater size in both cases (**1i** and **2i**) is almost neglectable compared to the size of the pre-heater and evaporator.

In case **B** (Point **3i** and **4i**), the largest heat exchange process is the liquid heat transfer process to the saturation curve. The heat transfer area in this process must be very high due to the higher evaporation temperature than in case **A**. The low temperature difference between the cold and hot flow to heat the liquid implies large areas in the heat exchange. The superheater size in (**3i**) and (**4i**) is also neglectable compared to the size of the pre-heater and evaporator.

294 As shown in Figure 8, the processes of evaporation and liquid heating are the most critical heat exchange pro-
295 cesses to the implementing of the RC and ORC configurations in a vehicle. The volume requirements for the RC
296 configuration with $dT=10^{\circ}C$ (**1i** and **3i**) could be too large for the implementation in a HDD engine. The ORC confi-
297 guration seems to be the solution with less technical restrictions from the point of view of volume requirements for the
298 heat exchangers. In steps (5) and (6) of Figure 1, an iterative process is specified; where dT has to be progressively
299 increased in order to fulfill the size due to packaging constraints in the vehicle. As we do not have any particular
300 vehicle with a particular packaging objective, we are going to skip such iterative process and straight forward propose
301 an increment of dT from $10^{\circ}C$ to $20^{\circ}C$ in order to exemplify its effect on reduction of $bsfc$. The configuration with
302 high temperature sources suffers a significant penalty of $bsfc$ in almost all the working points due to increase of dT .
303 Figure 9 shows the results of this study in the configuration with high temperature sources (case **B**) and ideal cycle
304 assumption. This figure shows a reduction of $bsfc$ improvements in the range of 8% to 4% for the ORC configuration,
305 and of 11% to 2% for the RC configuration.

306 Respect the condenser size, the new space requirement is practically negligible due to his place in the grille and
307 the high considered vehicle speed.

308 The effect of $dT=20^{\circ}C$ in the sizing of the heat exchanger is evaluated for the operating points with higher reduc-
309 tion of $bsfc$ for the RC and ORC configuration, i.e. 1800 rpm and 100% load for RC, and 1200 rpm and 50% load for
310 RC. These points are called as **5i** and **6i** respectively, as shown in Table 4. The results of these sizing problems are
311 shown in Figure 10. For both configurations with high temperature sources, a $dT=20^{\circ}C$ has implied a 50 % reduction
312 of the heat exchanger volume. Thus the volume requirements with $dT=20^{\circ}C$ are more acceptable. According to these
313 results, the ORC with the high temperature sources could be the solution easier to implement in a HDD engine taking
314 installation constraints into account.

315 The configuration with all sources (case **A**) practically does not produce a net power output. It is result of the low
316 temperature difference imposed between evaporator and condenser in order to recover the waste heat of cooling water.
317 This temperature difference is so low that it doesn't allow increasing the minimum temperature difference in the heat
318 exchangers (dT).

319 The condenser size in these two configuration is also negligible compared to the other evaporator and pre-heater.

320 3.7. Influences of real expander and pump

321 In this section, the effects of internal irreversibilities in the cycle output power are evaluated. These irreversibilities
322 are considered only in the expander and the pump. The pump model is simulated with a isentropic compression
323 efficiency of 80% [6]. The isentropic expansion efficiency of the turbine is determined using the turbine chart which
324 is referenced in [24]. In this chart, the optimal expander and the isentropic efficiency can be obtained from two
325 dimensionless numbers: the Load Number and the Flow Number. These coefficients are calculated though the inlet
326 and outlet conditions of the expander machine [25].

327 In the case **A** with all the heat sources and $dT = 10^\circ C$ an expansion ratio of 3 and 2 for RC and ORC respectively
328 is produced in the expander machine at all the operating points. The reason for these low expansion ratios is the low
329 evaporation temperature imposed, in order to recover the cooling water heat source. It allows an expansion process
330 completed with a single expander machine, obtaining an acceptable isentropic efficiency of 70%. Regarding the type
331 of expander, the chosen solution for RC is a reciprocating piston expander. In the ORC case, the expander can be a
332 radial or axial turbine.

333 On the other hand, in the case **B** with high temperature sources (EGR, exhaust gases and aftercooler), a high
334 expansion ratio is produced in the expander as shown in Figure 11. In the ORC results, the expansion ratio is higher
335 than in case **A** (6 vs 2). The optimal solution for this configuration using the turbine chart referenced in [24] is still an
336 axial or radial turbine with an isentropic efficiency of 70%. On the other hand, the expansion ratio in RC configuration
337 (25 with high temperature sources vs 3 with all sources) is too large to be efficiently implemented in a single stage
338 expansion. Thus, the optimal expander is a two-stage reciprocating piston expander with 70% and 60% of isentropic
339 efficiency for the first and second stage respectively.

340 The irreversibilities of the expander machine and the pump are imposed in the studied configurations.

341 Figure 12 shows the effects of the real compression and expansion processes in the four studied cases with
342 $dT=10^\circ C$. In the configuration with all sources, the irreversibilities of the expander machine are less critical, be-
343 cause the low expansion ratio provides the possibility of using a single stage expander. Now, the highest reduction
344 obtained in *bsfc* for the case **A** is limited to 10%, at 1200 rpm and 25% load both for RC and ORC solution. An even
345 greater impact on *bsfc* is obtained in the case **B** configuration with a maximum reduction of *bsfc* above 10% at 1800
346 rpm and 100 % load and 7% at 1200 rpm and 25% load for RC and ORC respectively.

347 Figure 13 shows the effects of the expander and pump irreversibilities with $dT=20^\circ C$ in the case **B**. The highest
348 reduction in this case is above 8 % at 1800 rpm and 100 % load for RC and 5 % at 1200 rpm and 25% load for ORC
349 solution.

350 The effect of the pump and expander irreversibilities in the heat exchanger inlet temperature is almost negligible.
351 For this reason, the volume requirements were considered equal to those in the ideal cycle study.

352 4. Summary

353 Table 6 is a summary showing the highlighted numerical results of the illustrative example exposed through this
354 paper. The table shows the performance and requirement at optimum solution for each operating point. Taking into
355 account the ideal cycle assumption, $dT = 10^\circ C$ and the configuration with all the sources (**A**), the bottoming cycle
356 reaches a maximum reduction of *bsfc* near 15% and 14%, for RC and ORC respectively (cases **1i** and **2i**). The case
357 **B**, with only the high temperature heat sources, ideal cycle and $dT = 10^\circ C$ can achieve a reduction near 14 % and
358 10% for RC and ORC respectively (cases **3i** and **4i**). The RC configurations need a high heat exchanger surface and

359 volume to run. The ORC configurations are therefore more technically feasible, due to the lower size requirements of
360 the heat exchangers.

361 The temperature difference between the hot and the cold flow (dT) dramatically affects to the reduction of $bsfc$. A
362 change from $dT = 10^{\circ}C$ to $dT = 20^{\circ}C$ reduces the size of the heat exchangers by about 50%, but this change also
363 increases the $bsfc$ by about 3 percentage points.

364 Finally, the results show that the irreversibilities in the expander and pump can lead to an increase between 2 and
365 4 percentage points the $bsfc$. In concrete terms, 3 percentage points of $bsfc$ increment in the most feasible case (**6r**)
366 with respect to the ideal (**6i**) case.

367 5. Conclusions

368 This paper describes a methodology to optimize a bottoming cycle which recovers low temperature waste heat
369 sources to generate mechanical power in vehicles. The methodology followed is to select the waste heat sources, the
370 optimum working fluid, the expander machine, the pump, the heat exchangers and the thermodynamic characteristics
371 of the cycle, according to different initial limitations or goals initially established. The goals are usually a reduction in
372 $bsfc$, with a low effect on the engine space requirements and low costs. In order to illustrate the methodology, the case
373 of an implementation of a bottoming cycle in a HDD engine has been described and a realistic result of a maximum
374 improvement of about 5 % in $bsfc$ has been obtained. In the heat sources selection, a power and exergy study of each
375 waste heat source is required in order to analyze which ones are the most useful for the generation of power output.
376 Taking different criteria into account, depending on the problem to solve, the optimal solution can be the recovering
377 of all the available heat sources or only the available heat sources with high temperature levels. Many heat sources to
378 recover imply high output power in the bottoming cycle but unfortunately, it also implies high heat exchanger volumes
379 and a complex control of the cycle and additionally, it can decrease the bottoming cycle average efficiencies.

380 The working fluid selection strongly affects to the performance of the bottoming cycle. Considering the case of
381 the HDD engine, the highest reduction in $bsfc$ is produced when the water RC is used. But these RC configurations
382 need high heat exchanger volumes to run. The ORC configurations are more technically feasible due to lower size
383 requirements of the heat exchangers (about 50% lower than RC configurations), but produce lower power than the RC
384 configurations (leading to differences of 3 percentage points in $bsfc$).

385 The minimum temperature difference in the heat exchangers (dT) dramatically affects the reduction of $bsfc$. So,
386 the heat exchanger sizing must be determined correctly to optimize the $bsfc$ with low space requirement. In the case
387 of the HDD engine, changing the dT from 10 °C to 20 °C leads to a decrease of the volume required by the heat
388 exchangers by about 60 % and increases the $bsfc$ by about 3 percentage points.

389 Therefore, considering the complexity of selecting the heat sources, the working fluid and the minimum temper-
390 ature difference in the heat exchangers, this paper presents an iterative methodology to obtain the goal defined in the

391 design of a bottoming Rankine cycle for a vehicle; with ground rules about the potential impact of the main design
392 assumption.

393 Finally, a literature review has been done to select the expander and the pump and analyze the effect of their
394 irreversibilities. Considering the case of a HDD engine, the expander obtained is a reciprocating piston expander for
395 RC and a radial turbine or axial turbine for ORC. The results show that these irreversibilities can involve an increase
396 between 2 and 4 percentage points in the calculated *bsfc*.

397 Therefore, considering the complexity of selecting the heat sources, the working fluid and the minimum temper-
398 ature difference in the heat exchangers, this paper presents an iterative methodology to obtain the goal defined in the
399 design of a bottoming Rankine cycle for a vehicle; with ground rules about the potential impact of the main design
400 assumption.

401 **6. Acknowledgements**

402 This work was partially funded by the "Programa de Formación de Profesorado Universitario (FPU)", "Programa
403 de Apoyo a la Investigación y Desarrollo de la Universidad Politécnica de Valencia 2010", "Proyectos I+D para grupos
404 de investigación emergentes 2011" and "Programa de apoyo a la investigación y desarrollo de la U.P.V (PAID-06-09)".
405 The authors thank J. Dahlqvist for his help in improving the English grammar.

References

- 406
407
- 408 [1] Pavlas M, Tous M, Bébar L, Stehlík P. Waste to energy- An evaluation of the environmental impact. *Applied Thermal Engineering* 2010;
409 20;2326-32.
- 410 [2] Ammar Y, Joyce S, Norman R, Wang Y, Roskilly AP. Low grade thermal energy sources and uses from the process industry in the UK.
411 *Applied Energy* 2012;89;3-20.
- 412 [3] Key World Energy Statistics. International Energy Agency 2008.
- 413 [4] Marrero GA. Greenhouse gases emissions, growth and the energy mix in Europe. *Energy Economics* 2010;32;135663.
- 414 [5] Keeling CD, Whorf TP. Atmospheric CO₂ records from sites in the SIO air sampling network. In *Trends: A compendium of data on global
415 change*. Technical Report, Oak Ridge National Laboratory, U.S. Department of Energy, Oak Ridge, Tenn, U.S.A., 2005.
- 416 [6] Chacartegui R, Sánchez D, Muoz JM, Sánchez T. Alternative ORC bottoming cycles FOR combined cycle power plant. *Applied Energy*
417 2009;86:2162-70.
- 418 [7] Wang J, Dai Y, Gao L. Exergy analyses and parametric optimizations for different cogeneration power plants in cement industry. *Applied
419 Energy* 2009;86:941-8.
- 420 [8] Bianchi M, Pascale AD. Bottoming cycles for electric energy generation: Parametric investigation of available and innovative solutions for
421 the exploitation of low and medium temperature heat sources, *Applied Energy* 2011;88;1500-9.
- 422 [9] Wei D, Lu X, Lu Z and. Gu J. Performance analysis and optimization of organic Rankine cycle (ORC) for waste heat recovery. *Energy
423 Conversion and Management* 2007;48:1113-9.
- 424 [10] Cayer E, Galanis A, Nesreddine H. Parametric study and optimization of a transcritical power cycle using a low temperature source. *Applied
425 Energy* 2010;87;1349-1357.
- 426 [11] Shengjun Z, Huaixin W, Tao G. Performance comparison and parametric optimization of subcritical Organic Rankine Cycle (ORC) and
427 transcritical power cycle system for low-temperature geothermal power generation. *Applied Energy* 2011;88;2740-2754.
- 428 [12] Roy JP, Mishra MK, Misra A. Performance analysis of an Organic Rankine Cycle with superheating under different heat source temperature
429 conditions. *Applied Energy* 2011;88;2995-3004.
- 430 [13] Algieri A, Morrone P. Comparative energetic analysis of high-temperature subcritical and transcritical Organic Rankine Cycle (ORC). A
431 biomass application in the Sibari district. *Applied Thermal Engineering* 2012 36;236-44.
- 432 [14] Garcia RF. Efficiency enhancement of combined cycles by suitable working fluids and operating conditions. *Applied Thermal Engineering*
433 2012, doi: 10.1016/j.applthermaleng.2012.02.039.
- 434 [15] Wang EH, Zhang HG, Fan BY, Ouyang MG, Mu QH. Study of working fluid selection of organic Rankine cycle (ORC) for engine waste heat
435 recovery. *Energy* 2012 36;3406-18.
- 436 [16] Eurostat, Statistical Office of the European Communities: Energy, transport and environment indicators. On the
437 web: <http://www.epp.eurostat.ec.europa.eu>.
- 438 [17] Morsy El Gohary M, Abdou KM. Computer based selection and performance analysis of marine diesel engine. *Alejadria Engineering
439 Journal* 2011;50;1-11.
- 440 [18] Arias DA, Shedd TA, Jester RK. Theoretical analysis of waste heat recovery from an internal combustion engine in a hybrid vehicle. *SAE
441 Paper* 2006;2006-01-1605.
- 442 [19] Teng H, Regner G. Improving fuel economy for HD Diesel Engines with EHR Rankine cycle driven by EGR cooler heat rejection. *SAE Paper*
443 2009;2009-01-2913.
- 444 [20] Ringler J, Seifert M, Guyotot V, Hübner W. Rankine cycle for waste heat recovery of IC engines. *SAE Paper* 2009;2009-01-0174.
- 445 [21] Dolz V, Novella R, García A, Sánchez J. HD Diesel engine equipped with a bottoming Rankine cycle as waste heat recovery system. Part 1:
446 Study and analysis of the waste heat energy. *Applied Thermal Engineering* 2011;36:269-78.
- 447 [22] Serrano JR, Dolz V, Novella R, García A. HD Diesel engine equipped with a bottoming Rankine cycle as waste heat recovery system. Part 2:
448 Evaluation of alternative solutions. *Applied Thermal Engineering* 2011;36:279-87

- 449 [23] Emission Standards for Model Year 2007 and Later Heavy-duty Highway Engines. U.S Environmental Protection Agency (EPA)
450 (<http://www.epa.gov/>).
- 451 [24] NSDS Turbine Chart Map.[cited 2012 Jan 20]. On the Web: www.barber-nichols.com/pdf/nsds_turbine_chart.pdf.
- 452 [25] Japikse D, Baines NC, (1997): Introduction to Turbomachinery. ETI, Inc. and Oxford, Oxford.
- 453 [26] Saleh B. Working fluids for low-temperature organic Rankine cycles. *Energy* 2007;32:1210-21.
- 454 [27] Angelino G, di Paliano PC. Organic Rankine Cycles (ORCs) for energy recovery from molten carbonate fuel cells. *Intersociety Energy*
455 *Conversion Engineering* 2000;2:1400-9.
- 456 [28] Drescher U. and Brüggemann D. Fluid selection for the Organic Rankine Cycle (ORC) in biomass power and heat plants. *Applied Thermal*
457 *Engineering* 2007;27:223-8.
- 458 [29] Serrano JR, Arnau FJ, Dolz V, Tiseira A, Lejeune M, Auffret N. Analysis of the capabilities of a two-stage turbocharging system to fulfil the
459 US2007 anti-pollution directive for heavy duty Diesel engines. *International Journal of Automotive Technology* 2008;9:277-88.
- 460 [30] Armstrong M. Basic Linear Geostatistics. Springer, Berlin ;1998.
- 461 [31] Surfer Version 8.0. Feb 11 2002.
- 462 [32] Energy and Exergy Balances for Modern Diesel and Gasoline Engines, Les recontrates scientifiques de l IFP- Advances in Hybrid Powertrains,
463 2008.
- 464 [33] Exergy analysis- a different perspective on energy- Part 2: rational efficiency and some examples of exergy analysis. SAE Technical Paper
465 904794,1990.
- 466 [34] Bourhis G, Leduc P, IFP. Energy and Exergy Balances for Modern Diesel and Gasoline Engines, Les recontrates scientifiques de l IFP-
467 Advances in Hybrid Powertrains, 2008.
- 468 [35] Tchanche BF, Lambrinos G, Frangoudakis A, Papadakis G. Exergy analysis of micro-organic Rankine power cycles for a small scale solar
469 driven reverse osmosis desalination system. *Applied Energy* 2010;87:1295-306.
- 470 [36] Badr O, Probert SD, O'Callaghan PW. Selecting a working fluid for a Rankine cycle engine. *Applied Energy* 1985;21:1-42.
- 471 [37] Yamamoto T, Furuhashi T, Ara N, More K. Design and testing of the Organic Rankine Cycle. *Energy* 2001;26:239-51.
- 472 [38] Duparchy A, Leduc P, Bourhis G, Ternel C. Heat Recovery for next Generation of Hybrid Vehicles: Simulations and Design of a Rankine
473 Cycle System. *World Electric Vehicle Journal* Vol 3. ISSN 2023-6653, 2009.
- 474 [39] Schuster A, Karellas S, Aumann R. Efficiency optimization potential in supercritical Organic Rankine Cycles. *Energy* 2010;35:1033-9.
- 475 [40] Nelson C. Exhaust Recovery Energy. In: 2008 DEER Conference, August 3rd, 2008
- 476 [41] Schuster A, Karellas S, Kakaras E, Spliethoff H. Energetic and economic investigation of Organic Rankine Cycle applications. *Applied*
477 *Thermal Engineering* 2009;29:1809-17.
- 478 [42] Shah RK, Sekulić DP. Heat Exchanger Design Procedures, in *Fundamentals of Heat Exchanger Design*. John Wiley and Sons, Inc, New
479 Jersey ;2003.
- 480 [43] Bell KJ. Delaware method for shell design, in: RK Shah, EC Subbarao, RA Mashelkar, editors. *Heat Transfer Equipment Design*, Washintong:
481 Hemisphere Publishing, p.145-66.
- 482 [44] Standards of the Tubular Heat Exchanger Manufactures Association, 8th edg (Tubular Heat Exchangers Manufactures Association New
483 York).
- 484 [45] Domingo JD. Analysis of complex assemblies of heat exchangers. *Int. J Heat Mass Transfer* 1969;12:537-48.
- 485 [46] Bhatti MS and. Shah RK. Turbulent and transition convective heat transfer in duct. *Handbook of Single-Phase convective Heat transfer*, New
486 York:Wiley;1987.
- 487 [47] Taborek J. Ideal tube bank correlations for heat transfer and pressure drop, in: EU Schlunder, editors. *Heat Exchanger Design Handbook*,
488 Washintong: Hemisphere Publishing;1983.
- 489 [48] Bromley LA. Heat transfer in stable film boiling. *Chemical Engineering Programe* 1950;46:221-7.
- 490 [49] Carey VP. Liquid-Vapor Phase-Change Phenomena: An Introduction to the Thermophysics of Vaporization and Condensation Process in
491 Heat Transfer Equipment, Taylor & Francis, Bristol; 1992.

- 492 [50] Ould Didi MB, Kattan N, Thome JR. Prediction of two-phase pressure gradients of refrigerants in horizontal tubes. *Int. J. Refrigeration* 2002;
493 25:716-30.
- 494 [51] Martinelli RC, Nelson B. Prediction of Pressure Drop during Forced-circulation Boiling Water. *Transaction of ASME* 1948; 70, 695-702.
- 495 [52] Ludwig EE. *Applied Process Design for Chemical and Petroleum Plants*, 3rd ed: Gulf Professional Publishing;2001.
- 496 [53] Kern DQ, *Process Heat Transfer*, New York: McGraw-Hill Book Co.;1950.
- 497 [54] Shah RK, Plate fin and tube-fin heat exchangers design procedures, in: Shah RK, Subbarao EC, Mashelkar RA editors. *Heat Transfer*
498 *Equipment Design*, Washintong: Hemisphere Publishing, p 225-66.

Nomenclature Acronyms

<i>BC</i>	Bryton Cycle
<i>bsfc</i>	Brake specific fuel consumption
<i>CFC</i>	Chlorofluorocarbon
<i>EGR</i>	Exhaust Gases Recirculation
<i>HCFC</i>	Hydrochlorofluorocarbons
<i>HFC</i>	Hydrofluorocarbons
<i>HDD</i>	Heavy Duty Diesel
<i>HFC</i>	Hydrofluorocarbons
<i>HP</i>	High Pressure
<i>IC</i>	Internal Combustion
<i>LP</i>	Low Pressure
<i>OCDE</i>	Organization for Economic Co-operation and Development
<i>ORC</i>	Organic Rankine Cycle
<i>RC</i>	Rankine Cycle
<i>SC</i>	Stirling Cycle

499

NOTATION

Latin

C_p	Heat capacity at constant pressure (kJ/kg.K)
C^*	Heat capacity rate ratio
D	Heat exchanger diameter (m)
dT	Minimum temperature difference in the heat exchanger ($^{\circ}C$)
E	Energy (kW)
Ex	Exergy (kW)
F	Log mean temperature difference correction factor
G	Mass flow velocity
h	Specific enthalpy (kJ/kg)
j	Ideal Coulburn heat transfer factor for the shell side
J	Correction factors of the heat transfer coefficient in the shell-side
L	Heat exchanger length (m)
L_x	Heat exchanger length in x direction (m)
L_y	Heat exchanger Length in y direction (m)

L_z	Heat exchanger length in z direction (m)
m	Mass flow (kg/s)
NTU	Number of transfer unit
Pr	Prandtl number
T	Temperature (°C)
rpm	Revolution per minute
s	Specific Entropy (kJ/kg.K)

Greek letters

Δ	Increment
μ	Viscosity

Subscripts

$flow$	Waste sources mass flow
s	Shell side
w	Wall conditions
0	Environmental condition
1	Inlet condition
2	Outlet condition

500

- 501 • listed of Tables
- 502 – Table 1. Operating points chosen for design bottoming cycle.
- 503 – Table 2. Energetic and exergetic levels for the waste heat sources at 1800 rpm - 100 % load and 1200 rpm-
- 504 25 % load.
- 505 – Table 3. Optimal bottoming cycle conditions at 1800 rpm -100 % load and 1250 rpm- 25 % load consid-
- 506 ering ideal cycle assumption for both configurations (Case **A** and Case **B**)
- 507 – Table 4. Bottoming cycle point chosen for the sizing of heat exchanger study.
- 508 – Table 5. Specification heat exchanger of points from **1i** to **4i**.
- 509 – Table 6. Summary of the optimum engine operating point for the considered configurations
- 510 • listed of Figures
- 511 – Figure 1. Flow chart for detailed methodology of preliminary design of a bottoming cycle for recovering
- 512 waste heat power in vehicles.
- 513 – Figure 2. HDD engine scheme.
- 514 – Figure 3. Total Waste Power in the HDD Engine (Stripped circles represent operating points experimen-
- 515 tally measured) .
- 516 – Figure 4. Total Waste Exergy in the HDD Engine (Stripped circles represent operating points experimen-
- 517 tally measured) .
- 518 – Figure 5. Exergy contribution of EGR, exhaust gases and aftercooler as a ratio of the total wasted exergy .
- 519 – Figure 6. Reduction rate of *bsfc* with an ORC/RC for the configuration with all the sources configuration
- 520 (case **A**).
- 521 – Figure 7. Reduction rate of *bsfc* with an ORC/RC for the configuration with high temperature sources
- 522 (case **B**).
- 523 – Figure 8. Volume requirements for the implementation of a bottoming cycle in four optimum operating
- 524 points selected in Table 2 .
- 525 – Figure 9. Reduction rate of *bsfc* in the configuration with high temperature sources (case **B**, $dT = 20^{\circ}C$
- 526 ideal cycle assumption).
- 527 – Figure 10. Volume requirements for the implementation of a bottoming cycle in two optimum operating
- 528 points selected in Table 2 .
- 529 – Figure 11. Expansion ratio in the expander machine for the configuration with high temperature sources
- 530 (case **B**) and $dT = 10^{\circ}C$

- 531 – Figure 12. Reduction rate of *bsfc* with real expander and pump with $dT = 10^{\circ}C$ for case **A** (Top) and case
532 **B** (Bottom).
- 533 – Figure 13. Reduction rate of *bsfc* with real expander and pump with $dT = 20^{\circ}C$ for case **B**.

Table 1: Operating points chosen for design bottoming cycle

Speed (rpm)	Load (%)
600	0
800	100
1000	100
	25
	50
1200	75
	100
	50
1500	100
	50
1800	100

Table 2: Energetic level for the waste heat sources at 1800 rpm - 100 % load and 1200 rpm- 25 % load

Speed (rpm)	Load (%)	Variable	EGR (kW)	Exhaust gases (kW)	Aftercooler (kW)	Intercooler (kW)	Cooling water (kW)	Total (kW)
1800	100	Power	75	147	21	30	151	424
		Exergy	40	60	5	4	26	135
1200	25	Power	16	53	10	4	51	134
		Exergy	6	20	1	0	8	35

Table 3: Optimal bottoming cycle conditions at 1800 rpm -100 % load and 1250 rpm and 25 % load considering ideal cycle assumption for both configurations (Case **A** and Case **B**)

Case	rpm	Load (%)	Cycle	Mass Flow (kg/s)	Condensation Temperature (°C)	Evaporation Temperature (°C)	Superheating Temperature (°C)
A	1800	100	ORC	2.40	50	71	80
			RC	0.20	50	70	177
	1200	25	ORC	1.37	50	71	71
			RC	0.10	50	70	159
B	1800	100	ORC	0.54	50	130	150
			RC	0.06	50	130	480
	1200	25	ORC	0.17	50	130	150
			RC	0.01	50	130	350

Table 4: Bottoming cycle point chosen for the sizing of heat exchanger study

Case Problem	Working fluid	<i>rpm</i>	Load (%)	Cycle	<i>dT</i> (°C)	Nomenclature of operating point
A	Water(RC)	1200	25	Ideal	10	1i
A	R245fa(ORC)	1200	25	Ideal	10	2i
B	Water(RC)	1800	100	Ideal	10	3i
B	R245fa(ORC)	1200	25	Ideal	10	4i
B	R245fa(ORC)	1200	25	Ideal	20	5i
B	R245fa(ORC)	1200	25	Ideal	20	6i

Table 5: Specification heat exchanger of points from **1i** to **4i**

Operating point	Heat Exchanger	Waste Source	Geometric specification	Pressure drop (Pa)	Volume (m^3)
1i	Pre-heater	Cooling water	L=0.4m ; D=0.7 m	35	0.049
	Evaporator	Aftercooler	L=6 m ; D=0.48 m	125	0.346
		Exhaust gases	L=9.6 m ; D=0.6 m	210	0.864
		EGR	L=0.6 m ; D=0.3 m	50	0.4239
	Superheater	EGR	Lx=0.1 m;Ly=0.05 m; Lz=0.05 m	279	0.005
2i	Pre-heater	Cooling Water	L=0.3m ; D=0.6 m	2634	0.027
	Evaporator	Aftercooler	L=2.8 m ; D=0.46 m	949	0.148
		Exhaust gases	L=2.64 m ; D=0.39 m	11000	0.100
		EGR	L=2.64 m ; D=0.2 m	3518	0.200
	Superheater	-	No Superheating	-	-
3i	Pre-heater	Intercooler	L=3.6m ; D=0.61 m	835	0.335
		Exhaust gases	L=5.4m ; D=0.83 m	1001	0.93
	Evaporator	Aftercooler	L=1.8 m ; D=0.27 m	107	0.0320
		Exhaust gases	L=3.6 m ; D=0.381 m	699	0.1300
		EGR	L=1.2 m ; D=0.27 m	313	0.01714
Superheater	EGR	Lx=0.07 m; Ly=0.05 m ; Lz=0.07 m	107	0.0003	
4i	Pre-heater	Intercooler	L=1.26 m ; D=0.61 m	1600	0.1172
		Exhaust gases	L=2.3m ; D=0.23 m	125	0.0304
	Evaporator	Aftercooler	L=1.8 m ; D=0.27 m	107	0.0320
		Exhaust gases	L=3 m ; D=0.34 m	699	0.1300
		EGR	L=2.3 m ; D=0.25 m	313	0.0171
Superheater	EGR	Lx=0.1 m; Ly=0.05 m ; Lz=0.01 m	307	0.0030	

Table 6: Summary of the optimum engine operating point for the considered configurations

CASE PROBLEM	Working Fluid	rpm	Load (%)	dT °C	Volume Requeriment(m^3)	Expander and pump	% reduction of <i>bsfc</i>	Nomenclature operating point
A (All Sources)	Water (RC)	1200	25	10	1.68	Ideal	15	1i
						Real	10	1r
	R245fa (ORC)	1200	25	10	0.48	Ideal	14	2i
						Real	10	2r
B (High Sources)	Water (RC)	1800	100	10	1	Ideal	14	3i
						Real	10	3r
				20	0.65	Ideal	10	5i
						Real	8	5r
	R245fa (ORC)	1200	25	10	0.27	Ideal	10	4i
						Real	7	4r
				20	0.17	Ideal	8	6i
						Real	5	6r

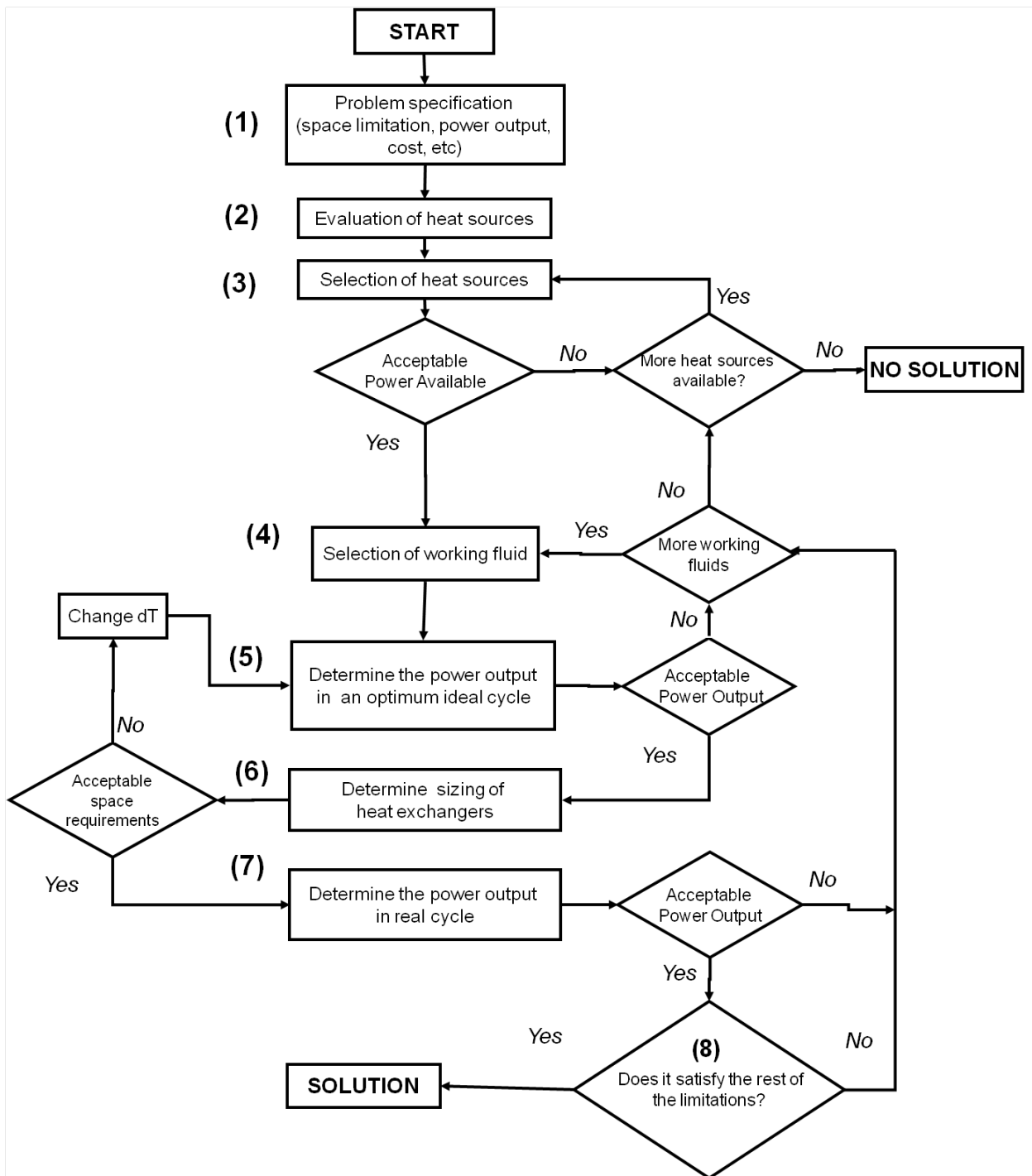


Figure 1: Flow chart for detailed methodology of preliminary design of a bottoming cycle for recovering waste heat power in vehicles

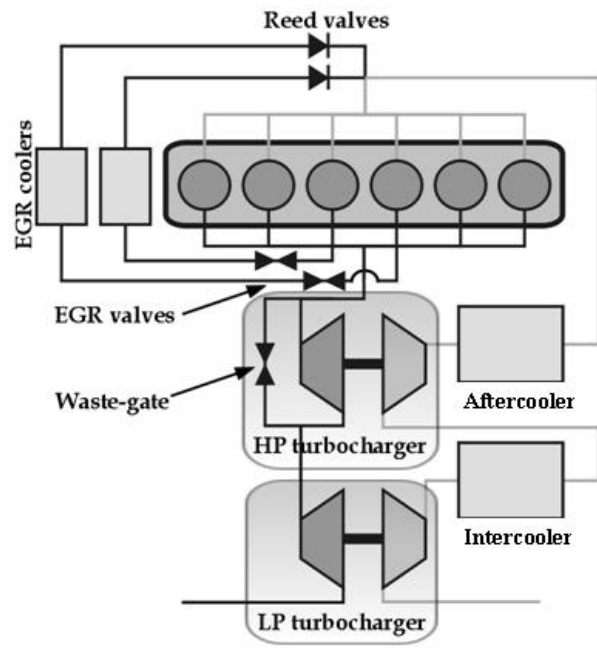


Figure 2: HDD engine scheme

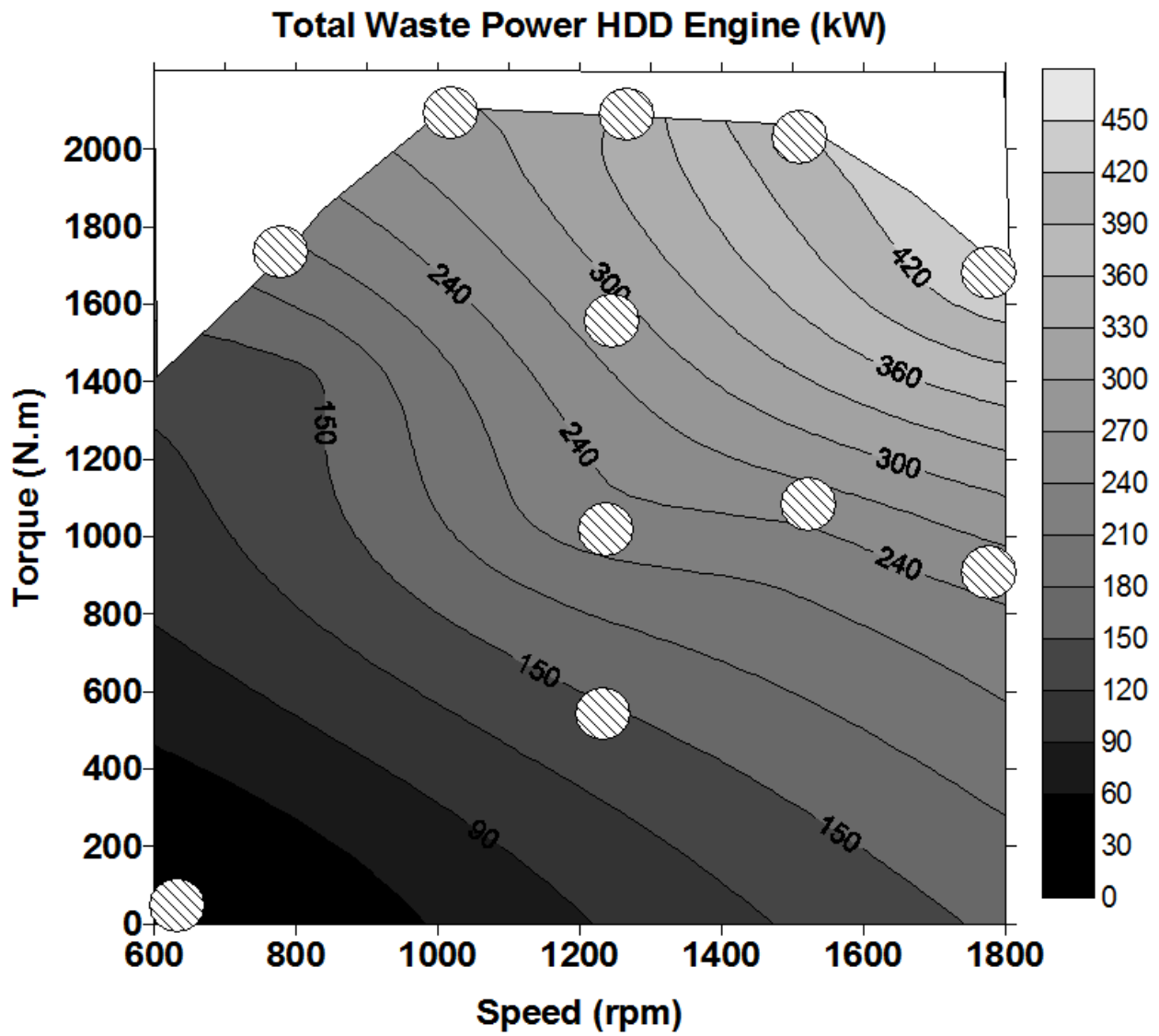


Figure 3: Total Waste Power in the HDD Engine (Stripped circles represent operating points experimentally measured)

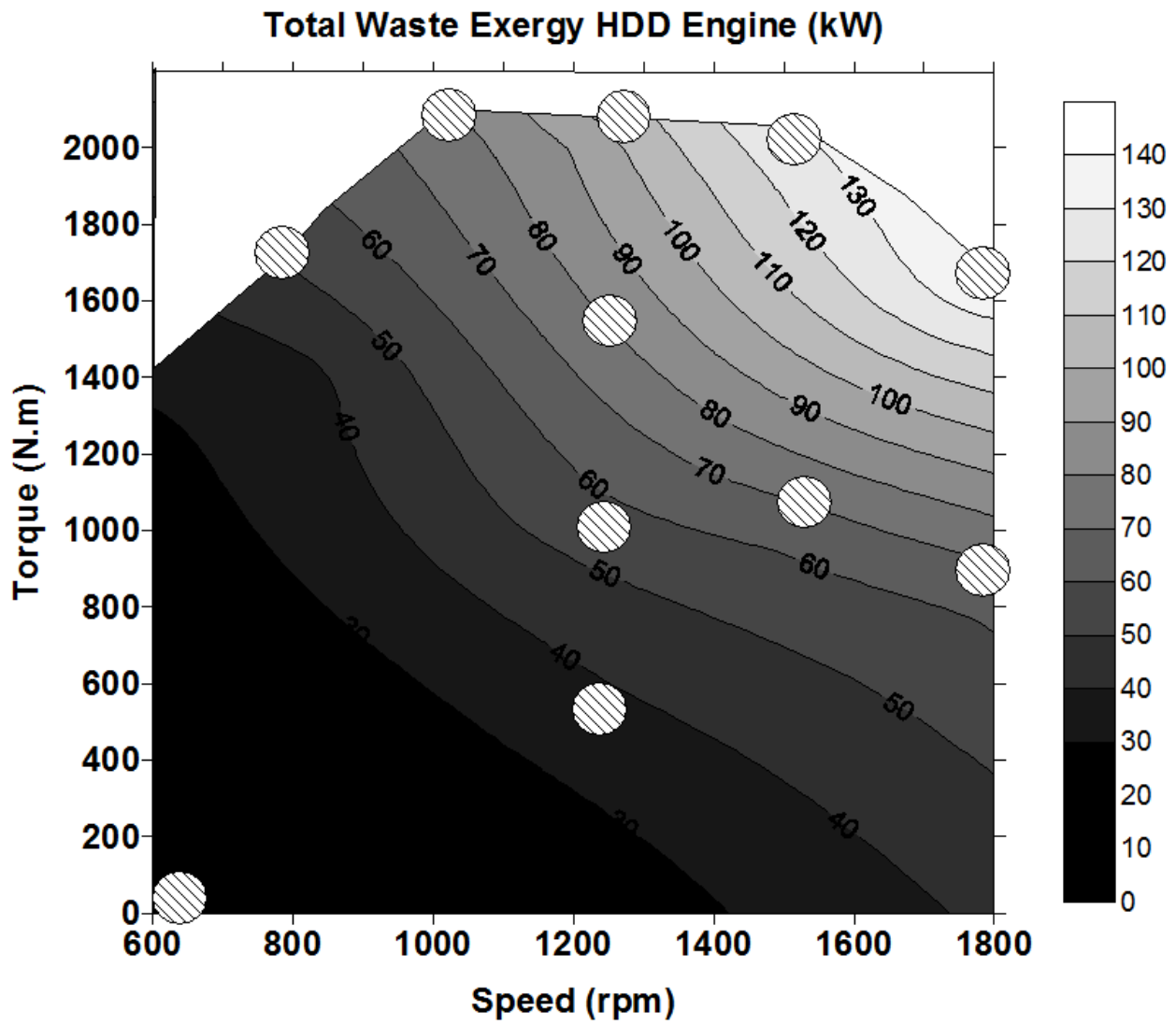


Figure 4: Total Waste Exergy in the HDD Engine (Stripped circles represent operating points experimentally measured)

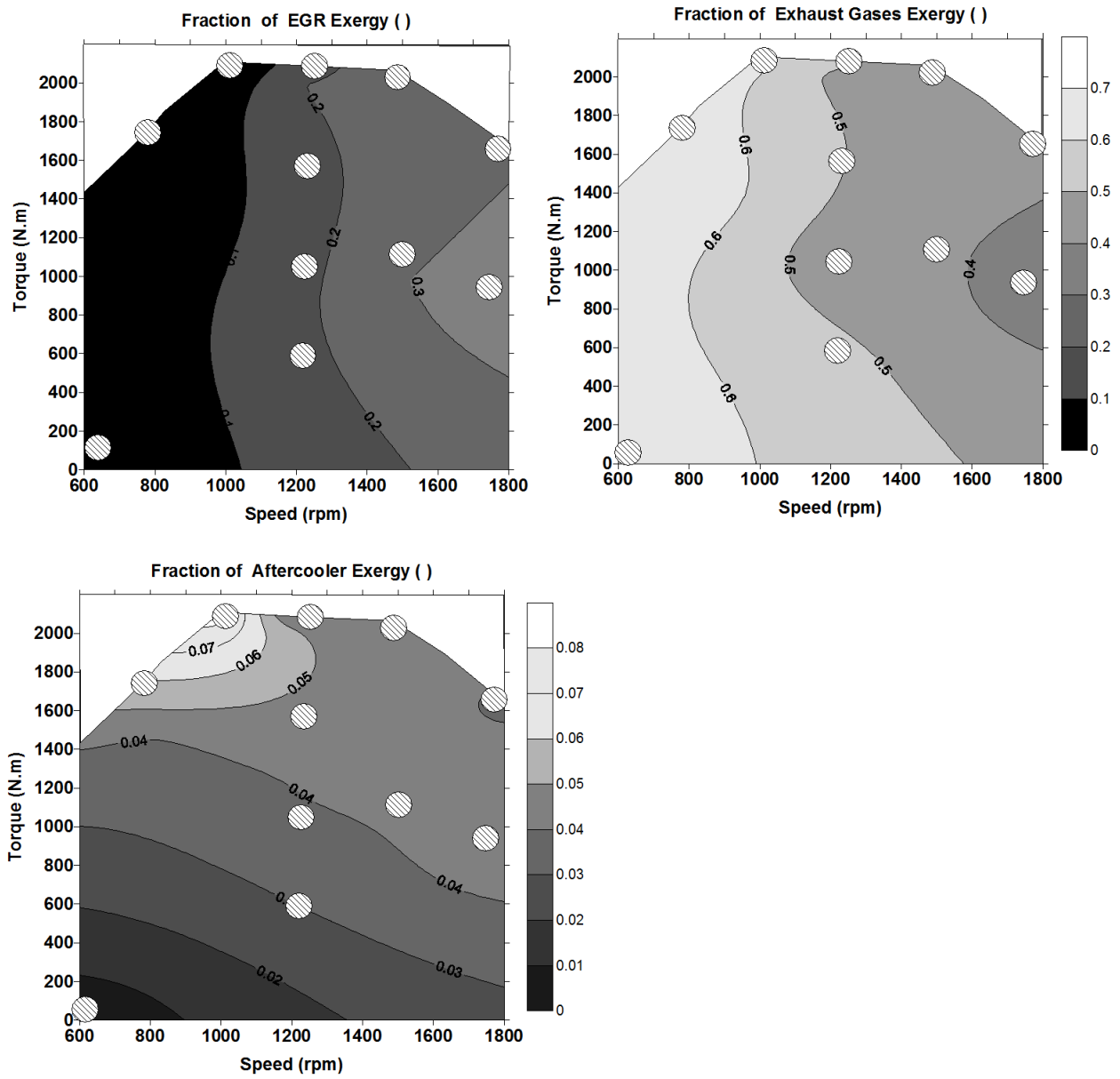
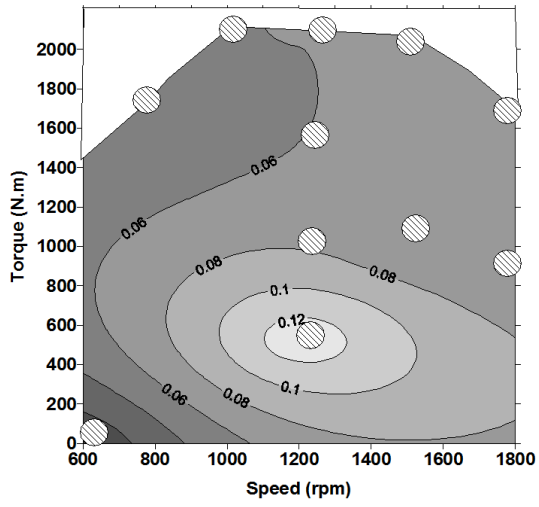


Figure 5: Exergy contribution of EGR, exhaust gases and aftercooler as a ratio of the total wasted exergy

Reduction rate of bsfc ORC (Configuration with all the waste sources)



Reduction rate of bsfc RC (Configuration with all the waste sources)

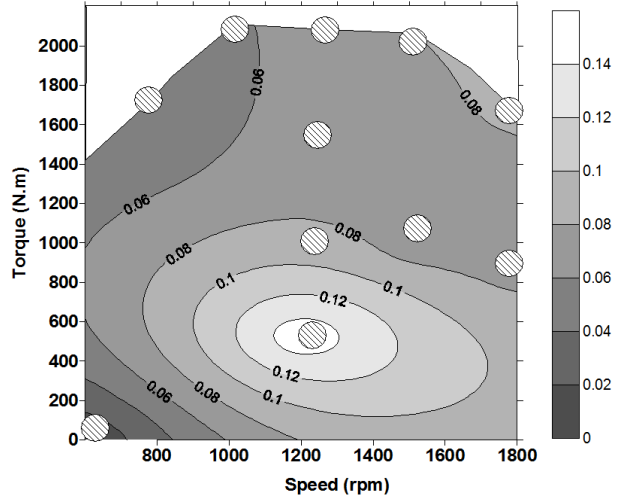


Figure 6: Reduction rate of *bsfc* with an ORC/RC for the configuration with all the sources configuration (case A)

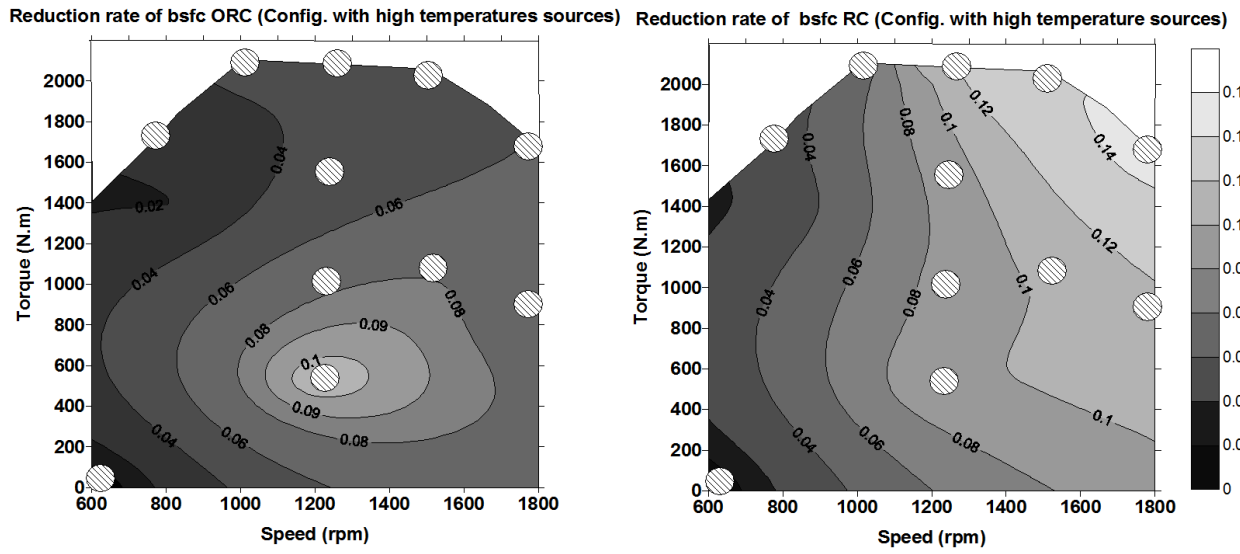


Figure 7: Reduction rate of *bsfc* with an ORC/RC for the configuration with high temperature sources (case **B**)

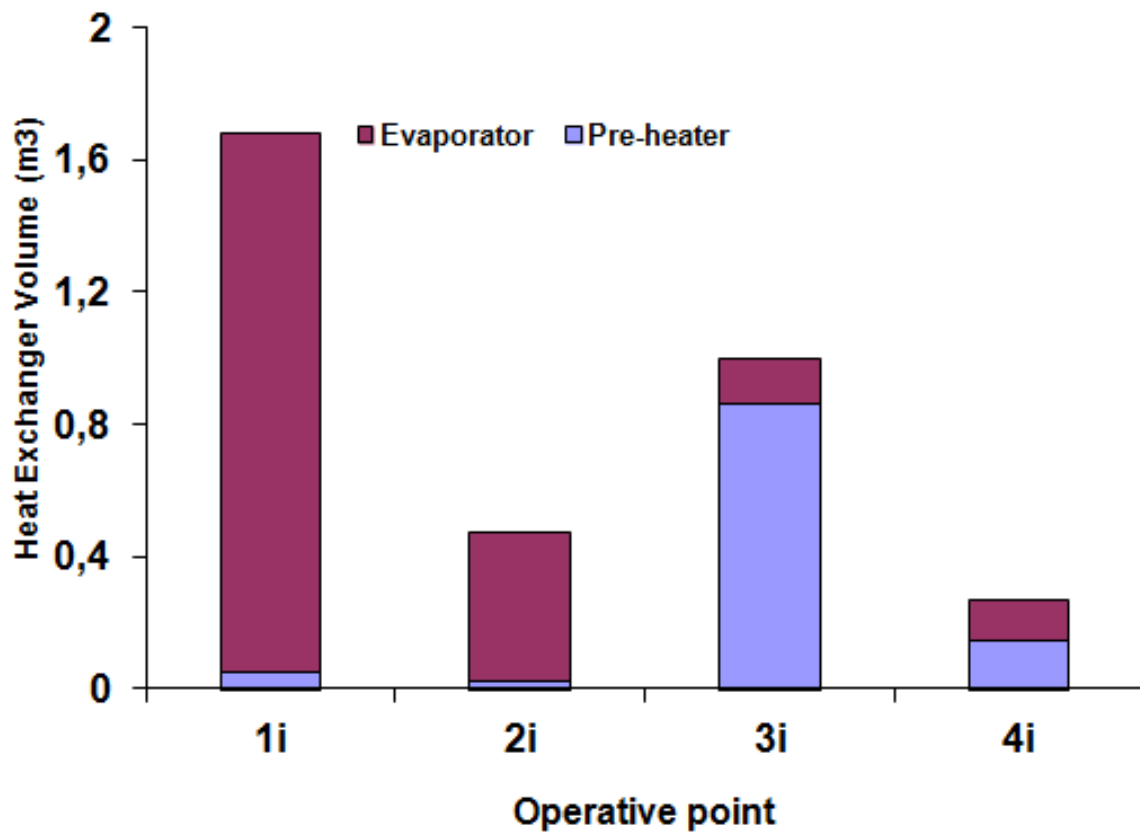


Figure 8: Volume requirements for the implementation of a bottoming cycle in four optimum operating points selected in Table 2

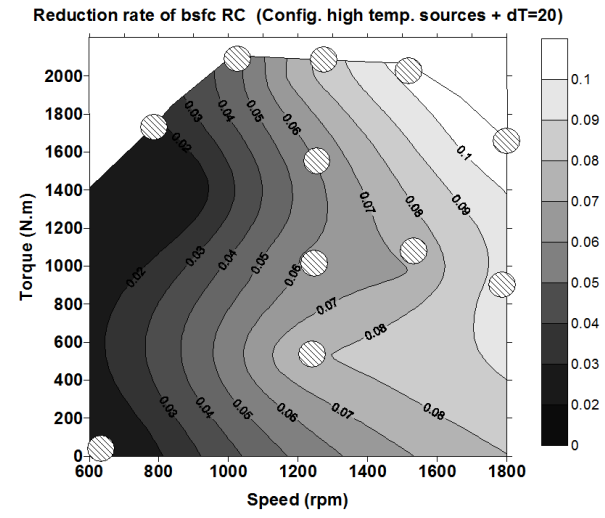
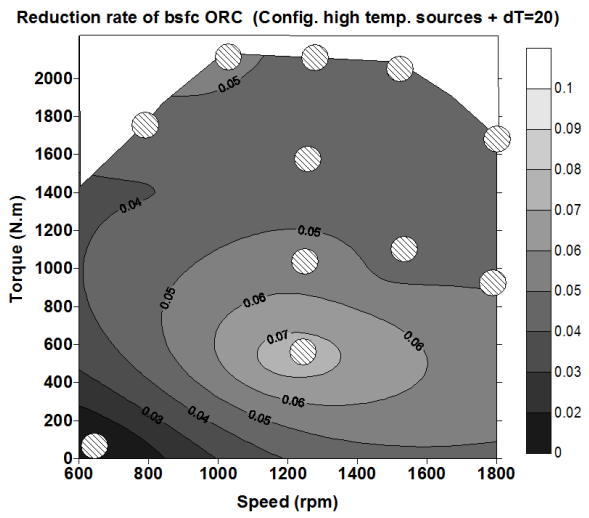


Figure 9: Reduction rate of *bsfc* in the configuration with high temperature sources (case **B**, $dT = 20^{\circ}C$ ideal cycle assumption)

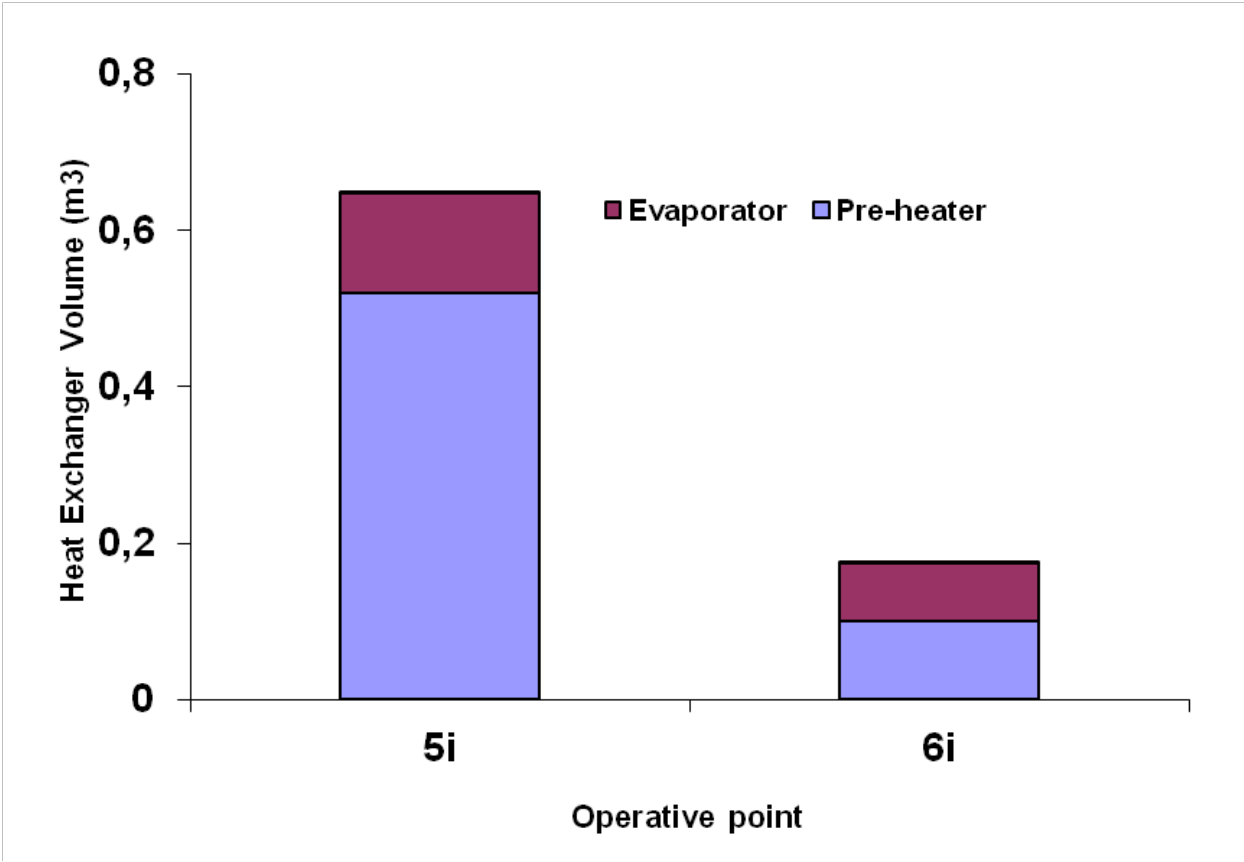


Figure 10: Volume requirements for the implementation of a bottoming cycle in two optimum operating points selected in Table 2

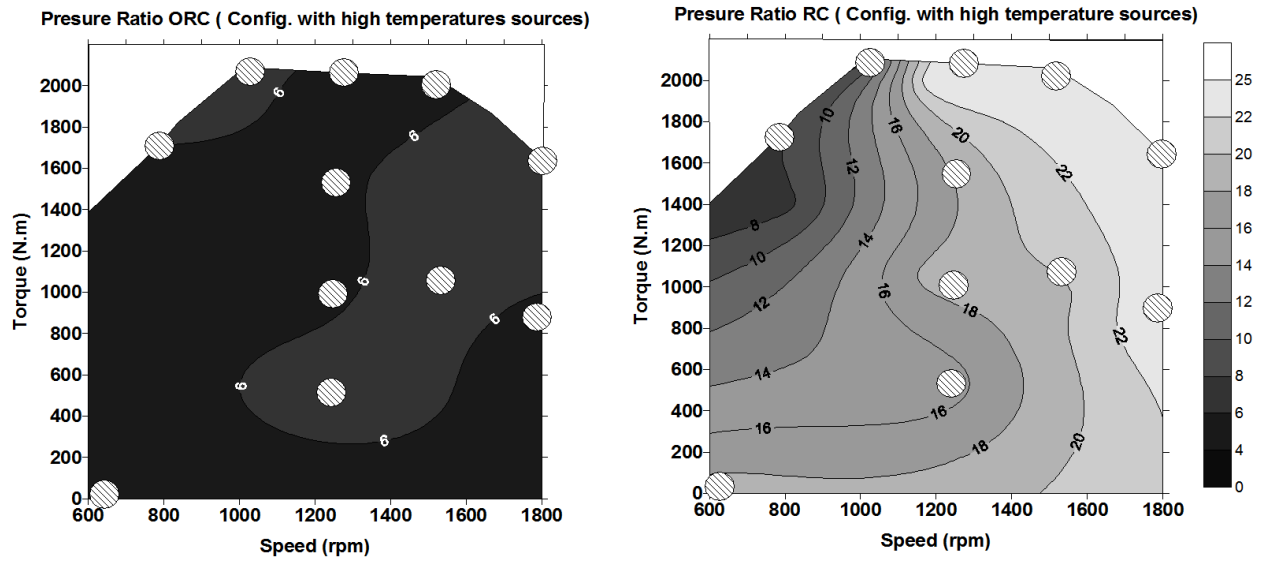
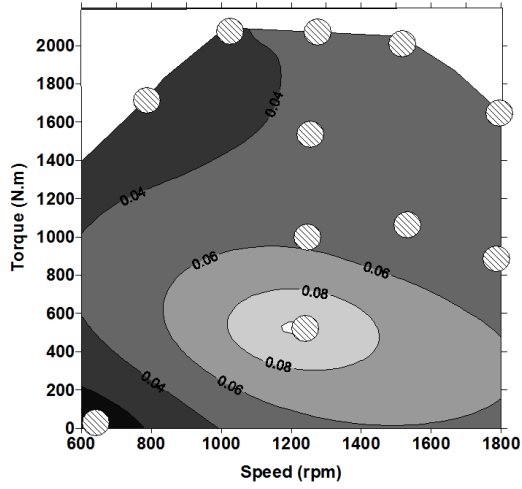
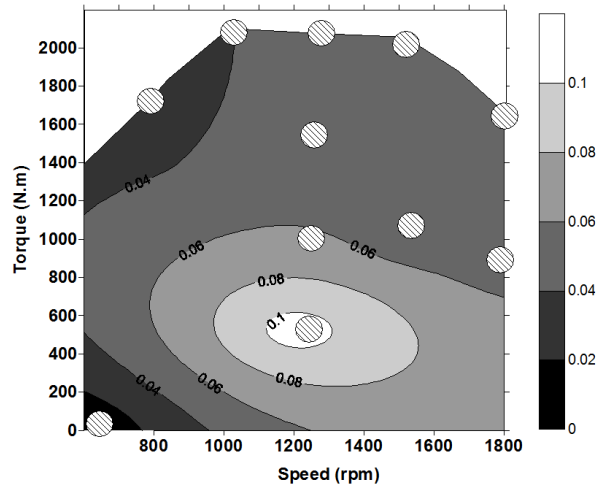


Figure 11: Expansion ratio in the expander machine for the configuration with high temperature sources (case **B**) and $dT = 10^{\circ}C$

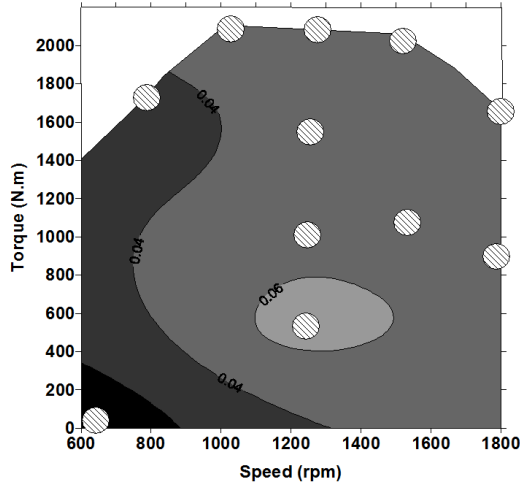
Reduction rate of bsfc ORC (Case A+dT=10+Real Expander and pump)



Reduction rate of bsfc RC (Case A+dT=10+Real Expander and pump)



Reduction rate of bsfc ORC (Case B+dT=10+Real expansor and pump)



Reduction rate of bsfc RC (Case B+ dT=10 + Real expansor and pump)

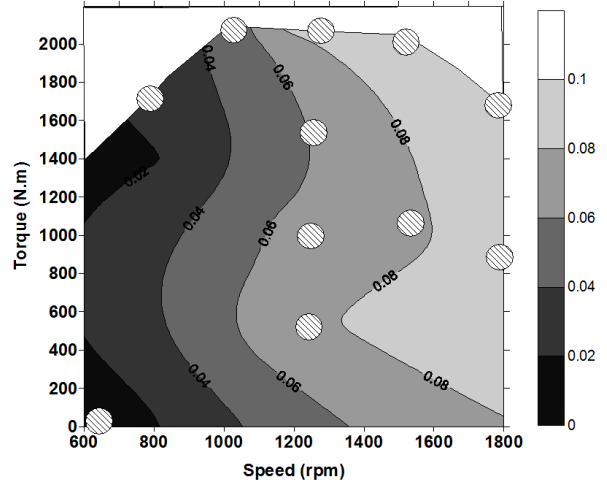


Figure 12: Reduction rate of *bsfc* with real expander and pump with $dT = 10^{\circ}C$ for case A (Top) and case B (Bottom)

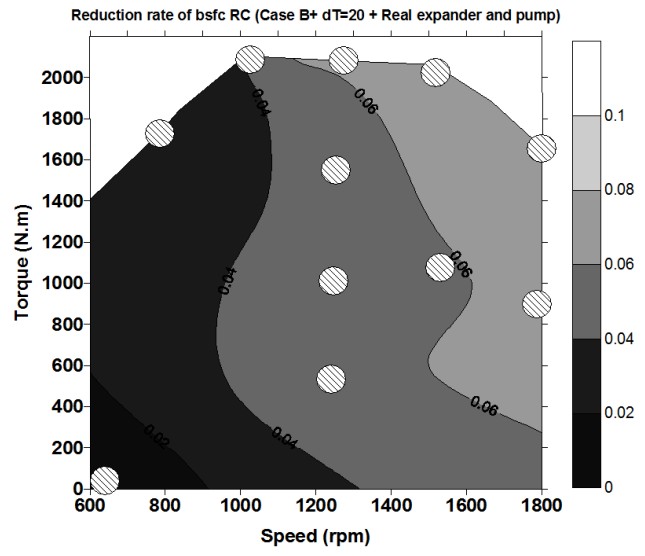
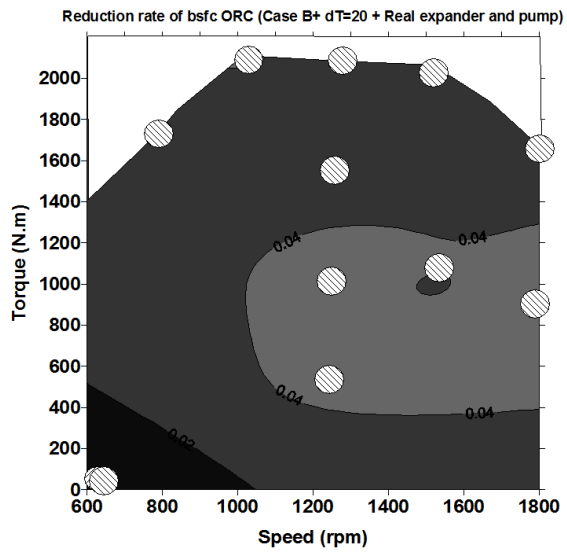


Figure 13: Reduction rate of *bsfc* with real expander and pump with $dT = 20^\circ C$ for case **B**